OPEN

Oncogene (2015) **34,** 5447–5459

www.nature.com/onc

ORIGINAL ARTICLE

Cytoplasmic p27 promotes epithelial–mesenchymal transition and tumor metastasis via STAT3-mediated Twist1 upregulation

D Zhao[1,2,8], AH Besser[1,2,8], SA Wander[1,2], J Sun[1], W Zhou[1,3], B Wang[1,3], T Ince[1,4], MA Durante[1,2], W Guo[5], G Mills[5], D Theodorescu[6] and J Slingerland[1,3,7]

p27 restrains normal cell growth, but PI3K-dependent C-terminal phosphorylation of p27 at threonine 157 (T157) and T198 promotes cancer cell invasion. Here, we describe an oncogenic feedforward loop in which p27pT157pT198 binds Janus kinase 2 (JAK2) promoting STAT3 (signal transducer and activator of transcription 3) recruitment and activation. STAT3 induces *TWIST1* to drive a p27-dependent epithelial–mesenchymal transition (EMT) and further activates AKT contributing to acquisition and maintenance of metastatic potential. p27 knockdown in highly metastatic PI3K-activated cells reduces STAT3 binding to the *TWIST1* promoter, *TWIST1* promoter activity and *TWIST1* expression, reverts EMT and impairs metastasis, whereas activated STAT3 rescues p27 knockdown. Cell cycle-defective phosphomimetic p27T157DT198D (p27CK-DD) activates STAT3 to induce a *TWIST1*-dependent EMT in human mammary epithelial cells and increases breast and bladder cancer invasion and metastasis. Data support a mechanism in which PI3K-deregulated p27 binds JAK2, to drive STAT3 activation and EMT through STAT3-mediated *TWIST1* induction. Furthermore, STAT3, once activated, feeds forward to further activate AKT.

Oncogene (2015) **34,** 5447–5459; doi:10.1038/onc.2014.473; published online 16 February 2015

INTRODUCTION

Metastasis is the leading cause of cancer-related death in most tumor types. Despite its devastating consequences, metastasis has long been recognized as an inefficient process in which cancer cells must overcome a series of challenges to spread from primary to distant sites.[1] Cancer cells must acquire the ability to invade locally, intravasate, extravasate and colonize organs to form distant metastases.[1] Local invasion, a critical event in which cancer cells dissociate from a primary tumor and invade surrounding stroma, involves reactivation of an embryonic developmental program referred to as the epithelial-to-mesenchymal transition or EMT. EMT is characterized by loss of E-cadherin (*CDH1*) expression via the upregulation of genes encoding *CDH1*-repressing transcription factors including *TWIST1*, *SNAI1* and *ZEB1*.[2] There is evidence that cancer cells recirculate after seeding to distant sites, and can reseed the primary tumor.[3] Thus, the EMT may be needed not only to initiate but also to maintain the metastatic process. A greater understanding of how EMT promotes invasion and metastasis may ultimately permit the design of more effective cancer therapies.

The present study provides novel evidence that the CDK inhibitor, p27, may acquire oncogenic potential to activate an EMT and drive subsequent metastasis. p27 was initially identified as a cyclin E-CDK2 inhibitor that mediates the G1-phase cell cycle arrest.[4–7] In keeping with its CDK inhibitory function, p27 knockout mice show increased body size, and p27 haploinsufficient mice are prone to carcinogen-mediated tumor formation, suggesting that p27 controls both tissue expansion and cell proliferation.[8–11] Loss of nuclear p27 is frequent in many human cancers and correlates with worse prognosis.[12] In contrast to other tumor suppressors such as p53 or p16, p27 is rarely deleted or fully lost in human cancer.[12] This is likely because p27 deregulation can confer pro-oncogenic gain of function. Although cell cycle inhibition is a nuclear function of p27, many cancers undergo pro-oncogenic changes when p27 is mislocalized to the cytoplasm.[12,13]

Deregulated, cytoplasmic p27 promotes tumor progression through the activation of cell motility and invasion.[14–16] In hepatocellular carcinoma cells, TAT-p27 protein transduction increased motility and cytoplasmic p27 colocalized with actin fibers to stimulate cell migration.[17] p27-null mouse embryonic fibroblasts have decreased motility that is rescued by either wild-type p27 or by a p27 mutant defective for cyclin and CDK binding (p27CK–), indicating that p27 effects on cell motility are independent of its cell cycle actions.[15] Cytoplasmic p27 can bind RhoA, impair RhoGEF action and reduce RhoA-ROCK signaling, leading to dynamic cytoskeletal rearrangements that increase cell motility.[15]

Here, we identify EMT-promoting effects of p27 that are driven by oncogenic PI3K pathway activation. Several PI3K effectors can phosphorylate p27 in the C terminus to shift its steady-state

[1]Braman Family Breast Cancer Institute at Sylvester Comprehensive Cancer Center, University of Miami Miller School of Medicine, Miami, FL, USA; [2]Sheila and David Fuente Graduate Program in Cancer Biology, University of Miami Miller School of Medicine, Miami, FL, USA; [3]Department of Biochemistry and Molecular Biology, University of Miami Miller School of Medicine, Miami, FL, USA; [4]Department of Pathology, Stem Cell Research Institute, University of Miami Miller School of Medicine, Miami, FL, USA; [5]Department of Bioinformatics and Computational Biology, and Department of Systems Biology, MD Anderson Cancer Center, Houston, TX, USA; [6]University of Colorado Cancer Center, University of Colorado, Aurora, CO, USA and [7]Department of Medicine, University of Miami Miller School of Medicine, Miami, FL, USA. Correspondence: Dr J Slingerland, Braman Family Breast Cancer Institute at Sylvester Comprehensive Cancer Center, University of Miami Miller School of Medicine, 1501 NW 10th Avenue, BRB708, Miami, FL 33136, USA.
Email: jslingerland@med.miami.edu
[8]Co-first authors.
Received 25 August 2014; revised 24 November 2014; accepted 19 December 2014; published online 16 February 2015

localization from the nucleus to the cytoplasm. Phosphorylation of p27 at threonine 157 (T157) by AKT[18–20] or SGK[21] impairs its nuclear import, whereas phosphorylation at T198 by AKT[22,23] or RSK[24,25] stabilizes cytoplasmic p27.[26,27] These C-terminal p27 phosphorylations appear to be processive and to promote binding and inhibition of RhoA-Rock to drive tumor invasion.[25] This may explain, in part, how activated Ras cooperates with p27CK− to induce murine tumorigenesis.[28] Indeed, our earlier work showed that a dual phosphatidylinositol 3-kinase/mammalian target of rapamycin (PI3K/mTOR) inhibitor could abrogate bone metastasis of a highly metastatic breast cancer line through restoration of nuclear p27.[29]

The present work reveals a novel mechanism whereby PI3K pathway activation and the accumulation of C-terminally phosphorylated p27 promote human tumor metastasis. We provide evidence that the C-terminal p27 phosphorylations at T157 and T198 confer a pro-oncogenic function to promote tumor metastasis by activating STAT3 (signal transducer and activator of transcription 3) to induce *TWIST1* and drive EMT. Highly metastatic phenotypes in breast and bladder cancer models were reversed by p27 knockdown and rescued in part by constitutively activated STAT3 (STAT3CA). These data provide a novel mechanism whereby p27 deregulation by oncogenic PI3K/mTOR activates pSTAT3 to drive human cancer progression. Pharmacological inhibition of signaling pathways that drive p27-mediated EMT may ultimately prove effective in preventing or reversing cancer metastasis.

RESULTS

Overexpression of phosphomimetic p27CK-DD induces/enhances EMT in human mammary epithelial and cancer cells

Prior work showed that mutations converting T157 and T198 to aspartate in p27 are phosphomimetic.[21,24,25] To test if negative charges at both sites cooperate to drive these effects, single and double phosphomimetic mutations (T157D, T198D or DD) were inserted into a p27 mutant that cannot bind either cyclins or CDKs (CK−) (Supplementary Figure S1A).[30,31] To test if C-terminally phosphorylated p27 may contribute early in the process of malignant transformation, these different phosphomutant p27 vectors were transduced into the immortalized, non-transformed human mammary epithelial cell line MCF-12A (MCF-12A-p27CK-DD). While the expression of each single phosphomimetic p27 mutant significantly increased cell migration, p27CK-DD enhanced MCF-12A migration most significantly and caused these cells to acquire the ability to invade matrigel (Figures 1a and b).

Similarly, in MDA-MB-231 cells, while p27CK− alone had a very modest effect, each phosphorylation site appears to contribute to cytoplasmic p27 localization and p27CK-DD caused the greatest increase in cell motility, invasion and p27 mislocalization (Supplementary Figures S1B–E). Neither p27CK− nor any of the CK− mutants bearing single or double phosphomimetic mutations affected the cell cycle (Supplementary Figure S1F). Relative levels of endogenous p27 and p27CK-DD are shown in Supplementary Figures S1G and H for the 231 model and in Supplementary Figures S2A and B for MCF-12A.

Notably, p27CK-DD-overexpressing MCF-12A cells underwent a progressive, morphological switch from a typical, cobblestone-like epithelial appearance to an elongated, spindle-like, mesenchymal shape over the next 4 weeks (Figure 1c), indicative of EMT. p27CK-expressing cells retained their cobblestone morphology, suggesting that the C-terminal phosphorylation of p27 is required for its action on the EMT (Figure 1c). p27CK-DD-overexpressing MCF-12A showed decreased levels of the epithelial marker, E-cadherin, and increased mesenchymal markers, N-cadherin and vimentin (Figures 1d, f). In MCF-12A cells, expression of vector alone or of the p27CK− vector lacking T157D and T198D mutations did not upregulate EMT drivers and mesenchymal markers (Supplementary Figure S2C). Thus, introduction of the CK− mutations and loss of cell-cycle inhibitory p27 function are not sufficient to drive p27-mediated EMT, and p27 phosphorylations at T157 and T198 appear to be required.

Similar findings were observed in the hTert-immortalized, normal human mammary epithelial HME3 line,[32] which showed a significant increase in mesenchymal marker expression, and enhanced cell migration and invasion following stable p27CK-DD transduction (Supplementary Figures S2D–G). Thus, overexpression of a p27 protein defective for CDK inhibition and bearing phosphomimetic mutations at T157 and T198 induces an invasive EMT phenotype in non-tumorigenic human mammary epithelial cells.

The EMT program is initiated by EMT-inducing transcription factors including Snail, Slug, zinc-finger E-box-binding homeobox 1 (Zeb1) and Twist.[33] To elucidate which transcription factors contribute to p27CK-DD-mediated EMT, several were screened by QPCR in MCF-12A-p27CK-DD and control cells. Although p27CK-DD modestly increased *SNAI1* (encoding Snail), *SNAI2* (encoding Slug) and *ZEB2* expression, *TWIST1* expression increased by 20-fold (Figure 1e), suggesting that *TWIST1* may have a critical role during p27CK-DD-induced EMT. p27CK-DD also increased Twist1 protein and its nuclear localization was confirmed by direct immunofluorescence (Figures 1d, f). Indeed, *TWIST1* knockdown significantly attenuated the EMT phenotype, causing re-expression of E-cadherin, loss of mesenchymal markers, N-cadherin and vimentin (Figure 1g), and loss of the excess motility and invasive potential of MCF-12A-p27CK-DD cells (Figures 1h and i), supporting the notion that *TWIST1* induction is a major driver of the p27CK-DD-induced EMT phenotype in immortalized human mammary epithelial cells.

p27CK-DD overexpression in the luminal A, MCF-7 breast cancer line also induced a morphological change compatible with EMT, with increased expression of mesenchymal markers (N-cadherin and vimentin) and *TWIST1*, and an increase in MCF-7 cell migration and invasion (Supplementary Figures S3A–E). Moreover, the effects of C-terminally phosphorylated p27 on EMT are not exclusive to breast cancer, as p27CK-DD significantly enhanced mesenchymal features of a human bladder cancer cell line, UMUC3 (Supplementary Figures S4A–E). Taken together, these data support a novel, oncogenic role in which p27 promotes EMT in human mammary epithelial cells and in weakly or non-metastatic breast and bladder cancer models.

Loss of p27 decreases mesenchymal characteristics in PI3K-activated metastatic lines

To assay if C-terminal phosphorylation of endogenous p27 contributes to EMT maintenance, the weakly metastatic MDA-MB-231 (231) breast cancer line and a derivative with enhanced lung metastatic ability, MDA-MB-231-4175 (4175)[34] were compared. In all, 4175 cells showed strong PI3K pathway activation: activating phosphorylations of AKT, SGK and PDK1 were increased while total kinase levels were similar and p27 was increased relative to parental 231 cells (Figure 2a). When equal amounts of cellular p27 were loaded from each line, 4175 cells showed a marked increase in both p27pT157 and p27pT198 compared with 231 cells (Figure 2b, upper panel). Subcellular fractionation followed by immunoblotting showed greater cytoplasmic p27 in 4175 cells compared with 231 cells (Figure 2b, lower panel). Stable p27 knockdown in 4175 increased E-cadherin, and decreased vimentin and Twist1 (Figures 2c and d). In 4175 cells, migration and matrigel invasion were both markedly decreased following p27 knockdown (Figure 2e). Stable p27 knockdown in 4175 cells did not alter cell cycle distribution (Figure 2f). Notably, small

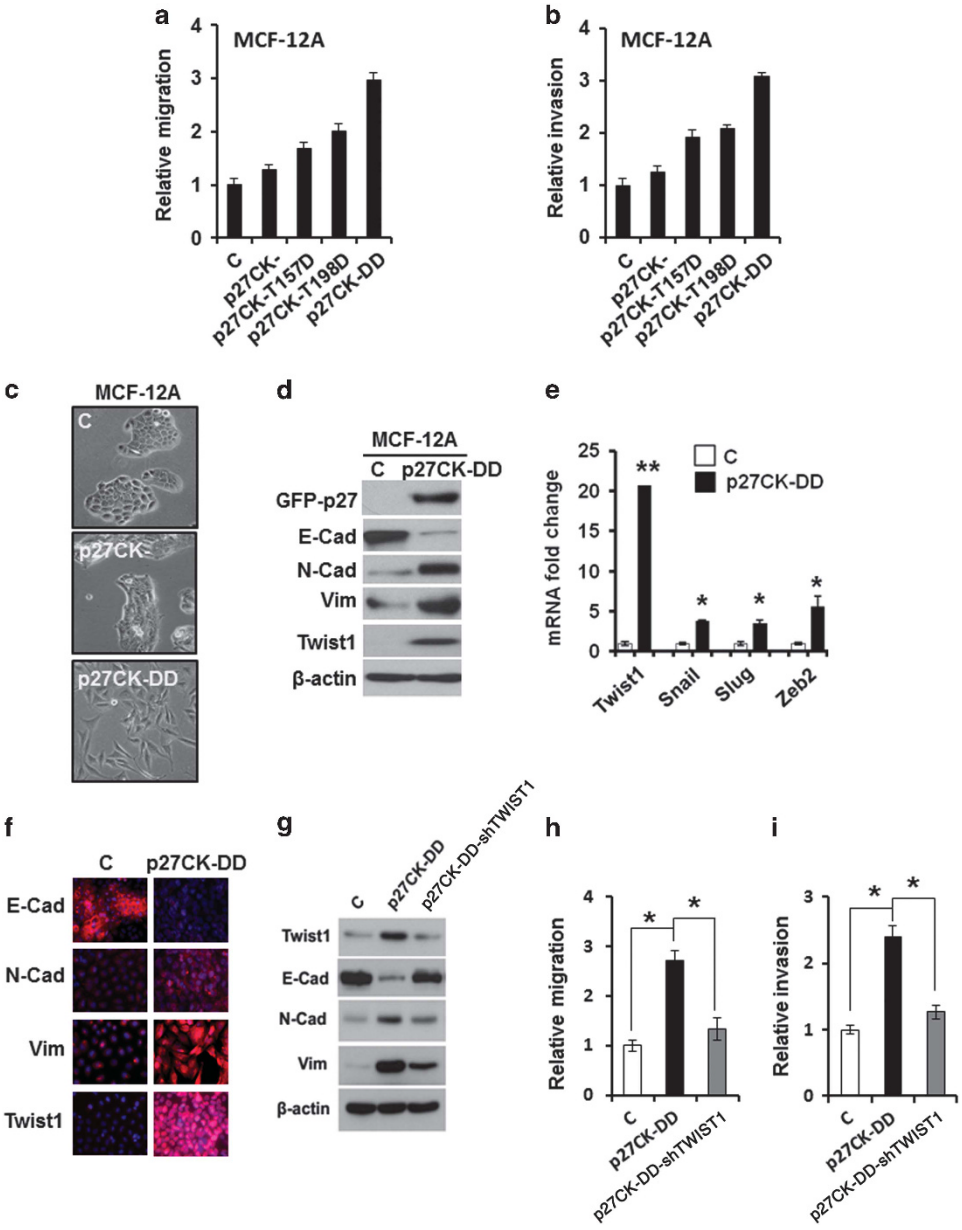

Figure 1. p27CK-DD overexpression induces EMT in immortal mammary epithelial cells. (**a** and **b**) MCF-12A was transduced with the indicated lentiviral p27 vectors and effects on migration and matrigel invasion are represented relative to vector-only controls. (**c**) MCF-12A were transduced with control vector, C, p27CK − or p27CK-DD and morphology demonstrated by phase-contrast microscopy. (**d–f**) MCF-12A were transduced with control vector, C, or p27CK-DD and compared as follows: western blot for EMT markers and *TWIST1* (**d**), QPCR for EMT transcription factors (**e**) and immunofluorescence for indicated proteins (**f**). (**g**) Effects of *TWIST1* knockdown on EMT markers in MCF-12A-p27CK-DD cells. (**h** and **i**) Transwell migration (**h**) and matrigel invasion (**i**) of MCF-12A-C and MCF12A-p27CK-DD are shown with or without *TWIST1* knockdown in MCF-12A-p27CK-DD. All data graphed represent mean of at least three repeats ± s.e.m. $^*P < 0.05$ by Student's *t*-test (also refer to Supplementary Figures S1–S3).

interfering (siRNA)-mediated p27 knockdown significantly reduced *TWIST1* expression within 8 h, followed by an increase in E-cadherin protein by 48 h (Figures 2g and h).

To validate these findings in a cancer from a different organ, we compared the UMUC3 bladder cancer line with a highly metastatic sister cell line, UMUC3-LuL2 (UMUC3-L), derived following selection and expansion of lung metastases from serial tail vein injections.[35] As in the breast cancer models, the highly metastatic UMUC3-L line showed significant PI3K pathway activation and increased p27 compared with parental UMUC3 (Figure 2i). Similarly, p27 knockdown significantly reduced mesenchymal characteristics, decreasing vimentin, N-cadherin and Twist1 expression (Figures 2j and k) and reduced cell motility (Figure 2l). Thus, in both metastatic breast and bladder cancer models with oncogenic PI3K activation, p27 appears to maintain an EMT program with increased cell motility and invasion.

p27CK-DD overexpression activates STAT3 to induce *TWIST1* and activate EMT

To elucidate the oncogenic signaling pathway(s) involved in p27CK-DD-induced EMT, we screened for signaling kinases known to contribute to EMT. Y705-phosphorylated and total STAT3 protein and *STAT3* mRNA were increased in MCF-12A-p27CK-DD cells compared with control MCF-12A (Figure 3a), as was nuclear STAT3 localization (Figure 3b). Nuclear STAT3 was minimal in

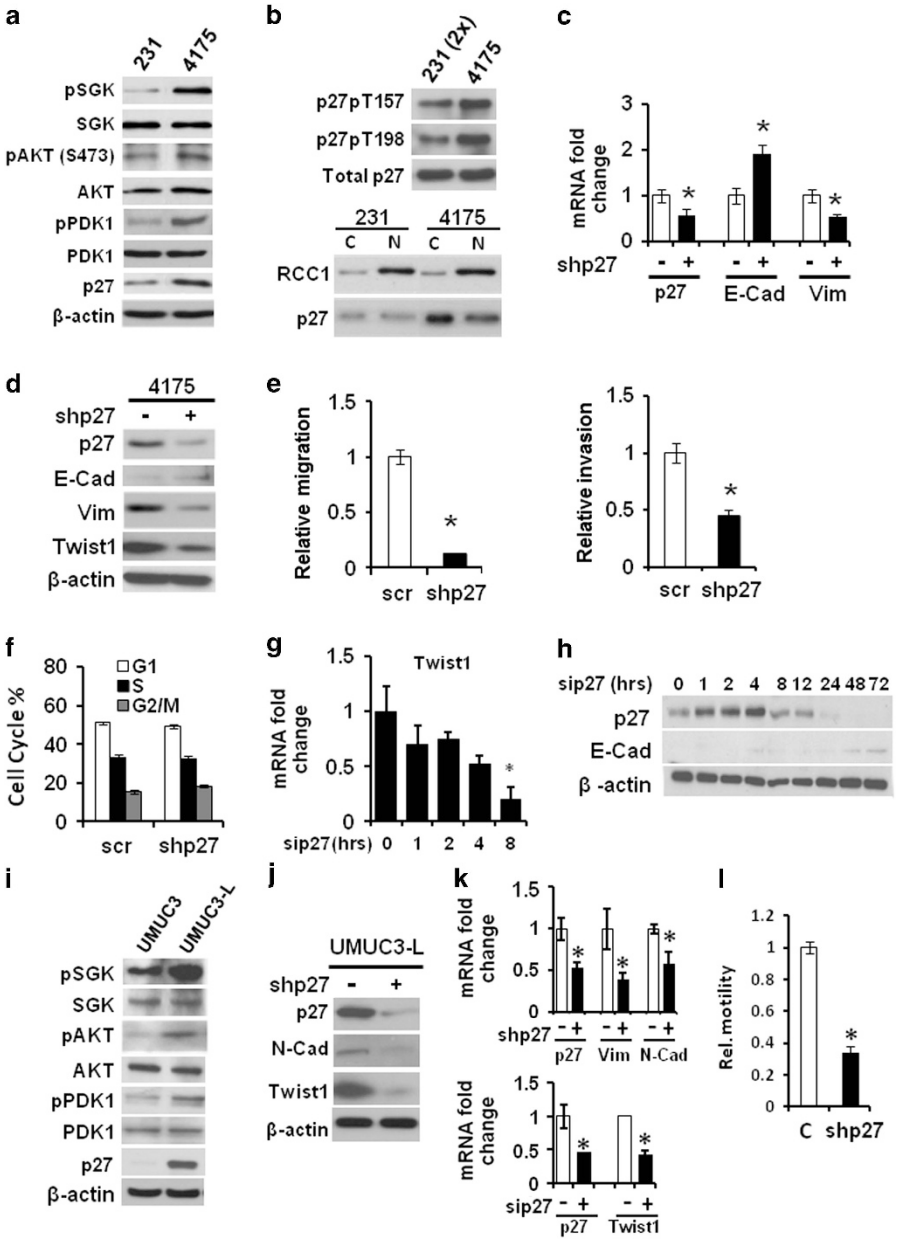

Figure 2. Loss of p27 reverts EMT in p27pT157pT198-enriched metastatic lines. (**a**) Western of PI3K activation and p27 in MDA-MB-231 (231) and MDA-MB-231-4175 (4175). (**b**) Lysates containing equal amounts of p27 were immunoprecipitated for p27pT157 or p27pT198 or total p27, and immunoblotted for p27 in 231 and 4175 cells (top). 2X indicates 231 protein lysate used was two times the amount used for 4175 cells. Fractionated lysates show p27 distribution in the nucleus, N, and cytoplasm, C, (bottom). (**c**–**f**) 4175 cells were transduced with shp27 (+) or sh-scramble controls (−) and compared as follows: QPCR for mRNA encoding p27, E-cadherin and vimentin (**c**), Western of p27 and EMT markers (**d**), Transwell migration (left) and transwell matrigel invasion (right) (**e**) and cell cycle distribution by flow cytometry (**f**). (**g**, **h**) The 4175 cells were transfected with sip27 and then assayed over the times indicated for *TWIST1* expression by QPCR (**g**), and p27 and E-cadherin expression by western blot (**h**). (**i**) Western blot of total and phosphorylated PI3K effector kinases in UMUC3 and UMUC3-LuL2 (UMUC3-L). (**j**–**l**) UMUC3-L cells with (+) or without (−) stable p27 knockdown (shp27) were compared by: western blot for indicated proteins (**j**), QPCR of p27, N-cadherin and vimentin (**k**, top). QPCR for *p27* and *TWIST1* mRNA in UMUC3-L cells treated with siRNA against p27 (+ sip27) or control oligo (−) (**k**, bottom). UMUC3-L cells with (+) or without (−) stable p27 knockdown (shp27) were assayed for transwell motility (**l**). All data graphed represent mean of at least three repeat ± s.e.m. $^*P < 0.05$ by Student's *t*-test compared with control.

control MCF-12A and in MCF-12A-p27CK-DD cells treated with an STAT3 inhibitor. Prolonged STAT3 inhibition over 2 weeks in culture reversed the mesenchymal phenotype of MCF-12A-p27CK-DD cells, shown by morphological change from spindle-shaped mesenchymal cells to a cobble-stone epithelial appearance (Figure 3b), increased E-cadherin and decreased mesenchymal markers and Twist1 expression (Figure 3c). STAT3 inhibitor treatment reduced the intense nuclear Twist1 expression in MCF-12A-p27CK-DD to levels seen in MCF-12A controls (Figure 3d). Interestingly, p27CK-DD overexpression markedly increased AKT activation, and this was attenuated by STAT3 inhibitor treatment (Figure 3e), suggesting that AKT activation in p27CK-DD is STAT3 dependent. Transduction of dominant-negative STAT3 (STAT3DN) into MCF-12A-p27CK-DD cells phenocopied pharmacological STAT3 inhibition, with reversion of EMT (Figure 3f), and marked attenuation of p27CK-DD-induced cell

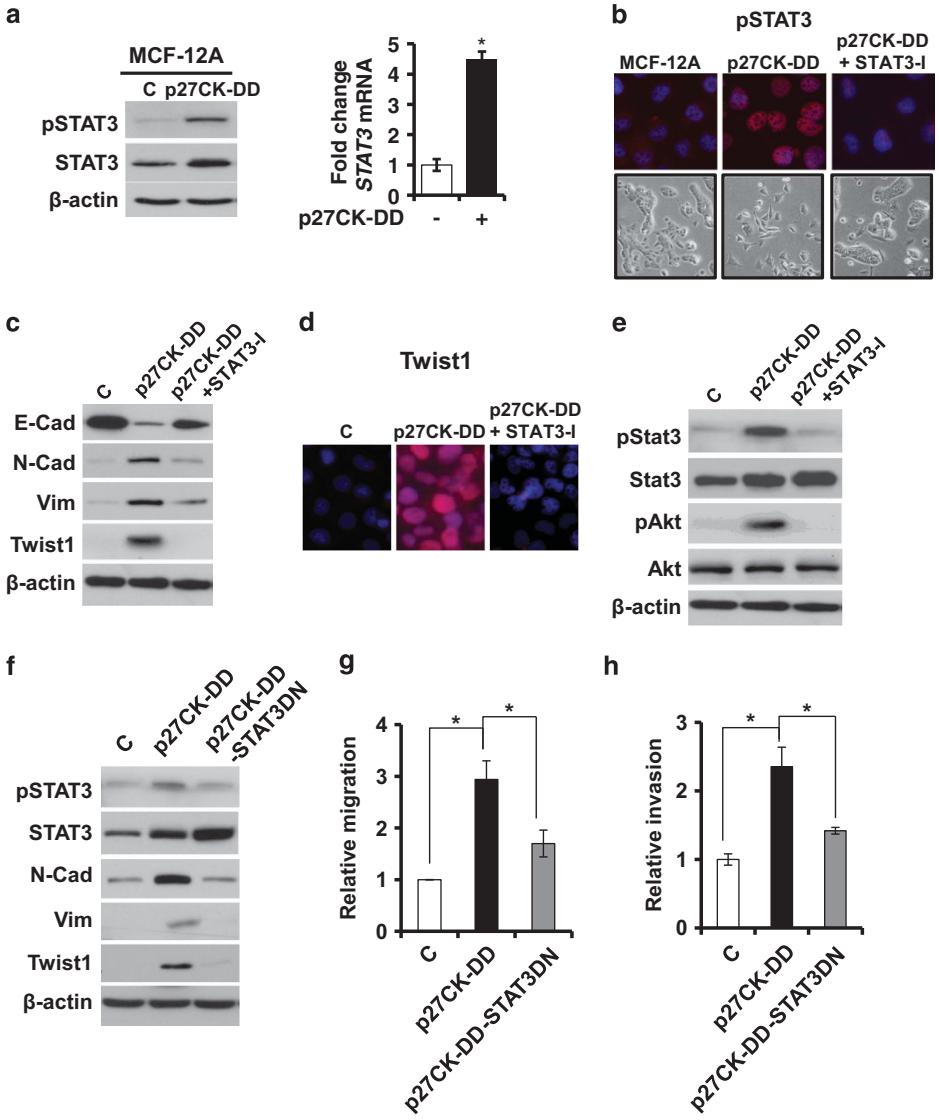

Figure 3. p27CK-DD drives STAT3 activation to induce EMT. (**a**) Western blot of pSTAT3 (Y705) and total STAT3 in vector control MCF-12A, C and MCF-12A-p27CK-DD (p27CK-DD) cells (left) and QPCR for *STAT3* mRNA in control MCF-12A and MCF-12A-p27CK-DD cells (right). (**b**) Immunofluorescence (top) and phase-contrast (bottom) images of pSTAT3 in control MCF-12A and MCF-12A-p27CK-DD cells with or without treatment for 2 weeks with STAT3 inhibitor (STAT3-I). (**c–e**) Control MCF-12A and MCF-12A-p27CK-DD cells treated with or without STAT3-I for 2 weeks were assayed for: Twist1 and EMT markers by western blot (**c**), Twist1 protein by indirect immunofluorescence (**d**) and total and activated STAT3 and Akt levels by western blot. (**f–h**) MCF-12A vector-only controls and MCF-12A-p27CK-DD cells with or without STAT3DN transduction were compared for Twist1 and EMT markers expression (**f**), transwell migration (**g**) and transwell invasion (**h**). All data are graphed as mean ± s.e.m. $^*P < 0.05$ by Student's *t*-test.

migration and invasion (Figures 3g and h). Thus, p27CK-DD-induced EMT is reversible in immortalized, non-malignant mammary epithelial cells and STAT3 signaling is critical for p27-dependent *TWIST1* induction and maintenance of this EMT phenotype.

p27 binds JAK2, increases JAK2-STAT3 complexes and enhances STAT3 transcriptional activity at the *TWIST1* promoter

We next assayed effects of p27 on transcriptional activity at the *TWIST1* promoter. As was the case for *TWIST1* expression (Figures 2d, g), *TWIST1* luciferase activity was also attenuated by p27 knockdown but not by scrambled short hairpin RNA controls (Figure 4a). Overexpression of STAT3-CA restored *TWIST1* promoter activity in p27 knockdown cells. STAT3 inhibition reduced *TWIST1* promoter activity in 4175 cells to the same extent as p27 knockdown (Figure 4a).

Quantitative chromatin immunoprecipitation (ChIP) assays revealed that STAT3 occupancy of the *TWIST1* promoter was increased in 4175 cells compared with 231 cells and attenuated by p27 knockdown, whereas p27CK-DD transduction increased STAT3 binding to the *TWIST1* promoter in 231 cells (Figure 4b). p27CK-DD expressing UMUC3 showed increased STAT3 binding to the *TWIST1* promoter and this was reversed by STAT3DN; and p27 knockdown in UMUC3-L decreased STAT3 occupancy of the *TWIST1* promoter (Figure 4c), supporting a model in which C-terminally phosphorylated p27 promotes STAT3 activation, driving STAT3 binding to the *TWIST1* promoter and *TWIST1* activation. Notably, ChIP assays failed to reveal co-occupancy of p27 with STAT3 on the *TWIST1* promoter.

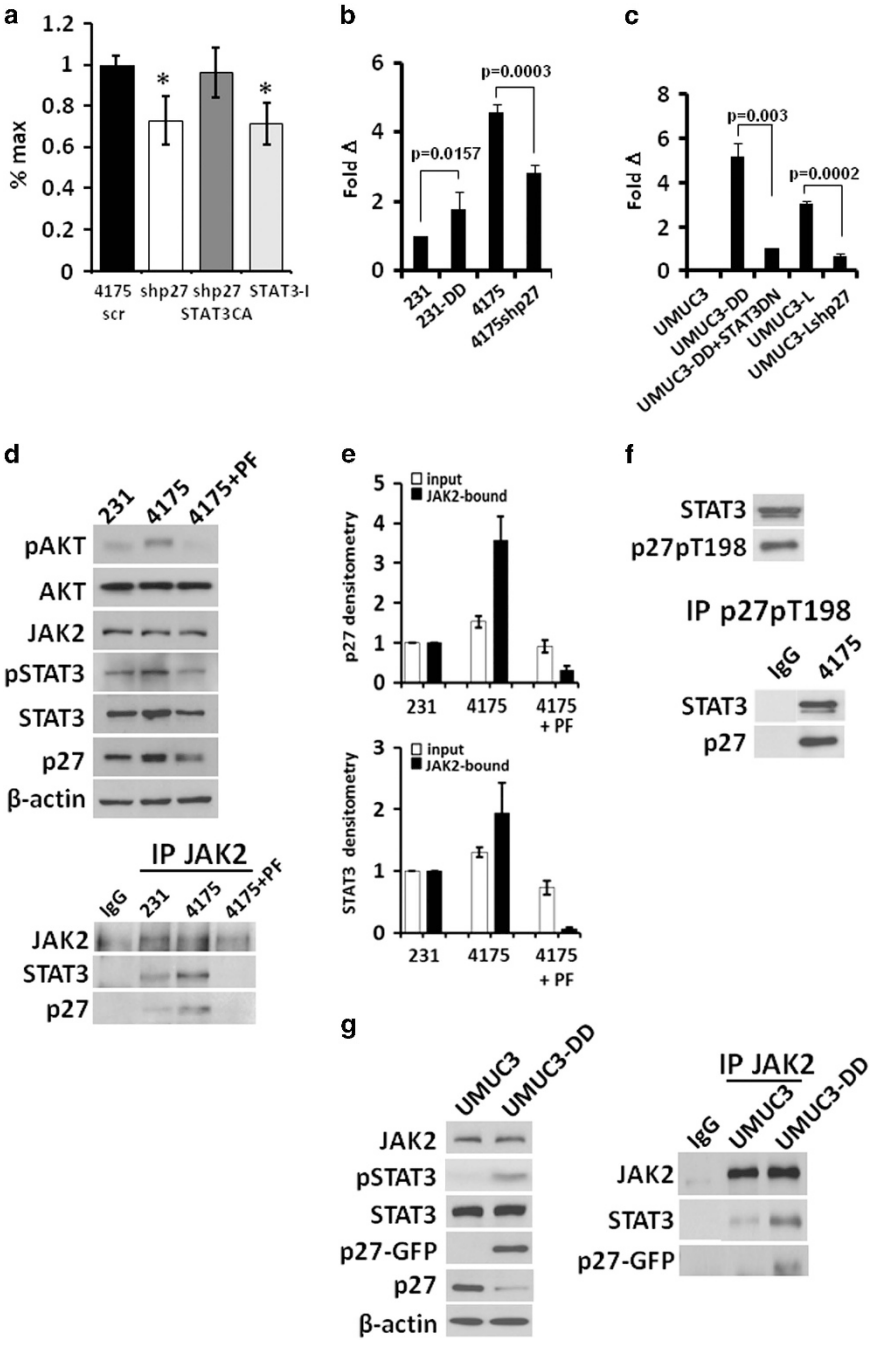

Figure 4. C-terminally phosphorylated p27 binds JAK2, increases JAK2-bound STAT3 and enhances STAT3 transcriptional activity at the *TWIST1* promoter. (**a**) Relative *TWIST1* promoter luciferase expression in 4175 scrambled shRNA controls (scr), 4175shp27 (shp27), 4175shp27+ STAT3-CA and 4175 treated with a STAT3 inhibitor (STAT3-I). (**b**) ChIP assays show relative STAT3 binding at the *TWIST1* promoter in 231, 231-p27CK-DD (231-DD), 4175 and 4175shp27 cells. (**c**) ChIP assays show relative STAT3 binding to the *TWIST1* promoter in parental UMUC3, UMUC3-p27CK-DD, UMUC3-p27CK-DD+STAT3DN, the highly metastatic variant UMUC3-LuL2 and in UMUC3-LuL2shp27 cells. (**d**) Immunoprecipitation of JAK2 in 231 and in 4175 cells treated with or without the PI3K/mTOR inhibitor PF1502 (PF) shows associated STAT3 and p27 (lower panel). Western blots show inputs (top panel). (**e**) Densitometry from (**d**) for both p27 (top) and STAT3 (bottom) comparing total protein (input) and protein bound to JAK2. (**f**) Western blots show input levels of STAT3 and p27pT198 in 4175 cells (top) and STAT3 bound to immunoprecipitated p27pT198 (bottom). (**g**) Western blots show input levels of JAK2, STAT3, p27-GFP and total p27 levels in UMUC3 and UMUC3-p27CK-DD cells (left). JAK2-associated STAT3 and p27-GFP were detected in JAK2 precipitates (right).

We next assayed if p27pT157pT198 might bind to JAK2-STAT3 (Janus kinase 2-STAT3) to promote STAT3 activation. p27 has been shown to bind JAK2 via both its catalytic and FERM domains.[36] Treatment of 4175 cells with a dual PI3K/mTOR inhibitor, PF-04691502 (PF), at 250 nM reduced pAKT to parental 231 levels by 48 h (Figure 4d, top panel). This drug dose, which reduces p27pT157 and p27pT198 levels,[29] also reduced total and activated STAT3, whereas JAK2 was unchanged (Figure 4d, top). Notably, JAK2-bound STAT3 and p27 were increased in 4175 cells compared with 231 cells (Figure 4d, bottom panel). Although total and activated STAT3 were modestly increased in 4175 cells compared with 231 and PF-treated 4175 cells, densitometric

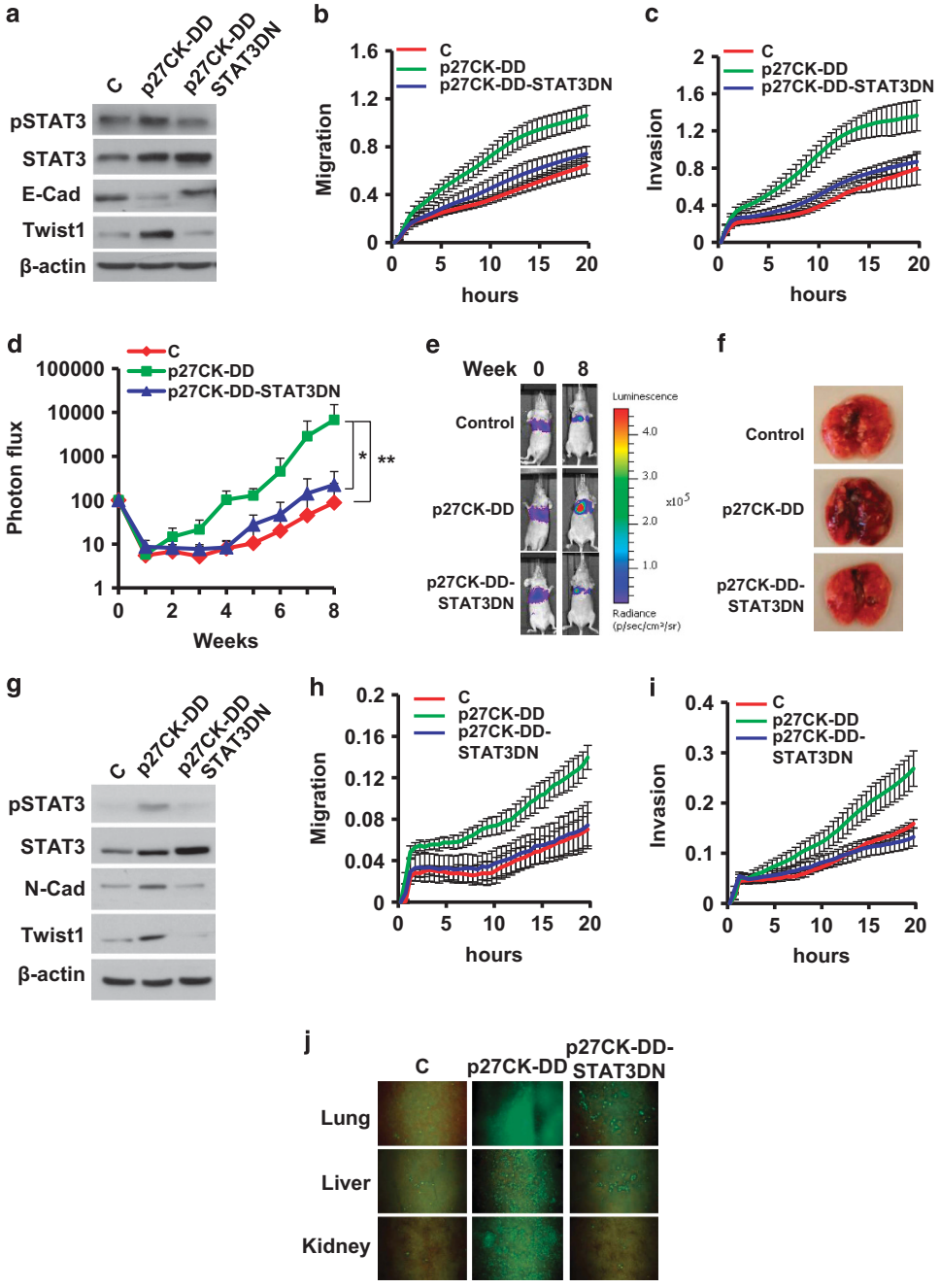

Figure 5. STAT3 inhibition decreases p27CK-DD-induced cancer metastasis. (**a–f**) The 231 cells were transduced with vector control, C, or p27CK-DD with or without STAT3DN, and the following were compared: protein levels by western blot (**a**), real-time migration (**b**), real-time matrigel invasion (**c**) and bioluminescence/time of experimental lung metastasis following tail vein injection (**d**), bioluminescence images of representative mice. The color scale depicts photon flux (photons/s) (**e**), gross morphology of tumor-bearing lungs (**f**). (**g–j**) UMUC3 cells were transduced with vector control or p27CK-DD with or without STAT3DN and the following were compared: protein levels indicated by western blot (**g**), real-time migration (**h**), real-time matrigel invasion (**i**) and representative immunofluorescence images of GFP-positive metastasis observed following tail vein injection in lungs, liver and kidney (**j**). Data are graphed as mean ± s.e.m. $*P < 0.05$ and $**P < 0.01$.

quantitation showed the increases in JAK2-bound STAT3 and p27 in 4175 cells were greater than predicted by their abundance alone (Figure 4e), suggesting that p27 binding may facilitate recruitment of STAT3 to JAK2. p27pT198 precipitation using a T198-phospho-specific antibody revealed associated STAT3 in 4175 cells (Figure 4f). Although these complexes were detected in 231, the p27pT198 and associated STAT3 levels were too low to permit accurate quantitation (not shown).

Notably, when p27CK-DD was stably expressed in the weakly metastatic UMUC3 bladder cancer line, a trimeric JAK2/p27CK-DD/STAT3 complex was detected. JAK2-bound STAT3 was increased and STAT3 was activated (Figure 4g).

STAT3 inhibition attenuates p27CK-DD-induced cancer metastasis

As both induction and maintenance of an EMT program are critical for metastatic tumor progression,[2,37,38] we next assayed effects of p27CK-DD overexpression with and without STAT3 inhibition on invasion and metastasis in our breast and bladder cancer models. p27CK-DD transduction into 231 cells increased STAT3 levels and

STAT3 activation, increased Twist1, decreased E-cadherin (Figure 5a) and markedly increased cell migration and invasion (Figures 5b and c) over control 231 cells. Transduction of STAT3DN into 231-p27CK-DD cells reverted the mesenchymal phenotype, causing loss of Twist1, increased E-cadherin and reversed the p27-driven increase in cell migration and invasion (Figures 5a–c).

Upon tail vein injection into nude mice, both the number and size of lung metastasis formed from p27CK-DD-expressing 231 cells were significantly increased, as was cumulative tumor bioluminescence compared with parental 231 controls (Figures 5d and f). The p27CK-DD-mediated gain of metastatic potential was STAT3 dependent: STAT3DN transduction attenuated lung tumor formation by 231-p27CK-DD cells to levels similar to those of parental 231 (Figures 5d–f).

The prometastatic effect of p27CK-DD was confirmed in the UMUC3 bladder cancer model. p27CK-DD overexpression in UMUC3 parental cells activated STAT3, modestly increased STAT3 mRNA and induced a STAT3-dependent increase in N-cadherin and Twist1, and increased cell migration and invasion (Figures 5g–i and Supplementary Figure S4F). Moreover, p27CK-DD overexpression caused widespread multiorgan tumor metastasis *in vivo*, detected by direct immunofluorescence of metastatic tumor that was not observed in parental UMUC3, and this was attenuated by coexpression of STAT3DN (Figure 5j). These data provide strong evidence that STAT3 activation is required for p27CK-DD-induced EMT and enhanced metastasis in these models.

p27 knockdown reduces metastasis *in vivo* and this is reversed by STAT3-CA

As loss of p27 reversed the EMT phenotype in the highly metastatic 4175 and UMUC3-L (Figure 2), we next assayed effects of p27 knockdown on their metastatic potential *in vivo*. In 4175 cells, p27 knockdown markedly reduced pSTAT3 and caused a modest decreased in *STAT3* mRNA and protein levels (Figures 6a and c). This is consistent with the known action of pSTAT3 to transactivate the *STAT3* gene. An increase in *STAT3* mRNA expression was also observed in p27CK-DD- transduced cells (Figure 3a and Supplementary Figure S4F). Similarly, in UMUC3-L, p27 knockdown decreased pSTAT3 (Figure 6g). As observed *in vitro* for cell migration and invasion (Figure 2), loss of p27 also significantly decreased experimental lung metastasis formed by both 4175 ($P < 0.001$) and UMUC3-L cells ($P < 0.001$) (Figures 6d–f and h–j). The loss of metastatic ability could not be attributed to a cell-cycle effect for either cell model (Figure 2f and Supplementary Figure S5). Since STAT3 activity was decreased by p27 knockdown, a STAT3-CA was introduced into 4175shp27 cells to test if restoration of STAT3 activity could rescue the loss of metastasis caused by p27 knockdown. In 4175shp27 cells, STAT3-CA expression partially restored loss of metastasis following p27 knockdown (Figures 6d–f), suggesting that STAT3 serves as a critical mediator of the prometastatic effects of p27pT157pT198 *in vivo*.

p27pT157 correlates with STAT3 and PI3K/mTOR activation

Proteomic analysis of 747 primary human breast cancers from The Cancer Genome Atlas (TCGA)/The Cancer Proteome Atlas (TCPA) data set showed that p27pT157 and p27pT198 are highly correlated (correlation coefficient $R = 0.411$, $P = 0$) and both are strongly associated with the activation of kinases downstream of PI3K, p70pT389, p90pT359, S6pS235 and S6pS240 ($R = 0.13$–0.41, all P-values $< 9E-08$) and correlate negatively with PTEN ($R = -0.24$, $P = 8.9E-11$ and $R = -0.14$, $P = 0.0002$, respectively) (data shown for p27pT157 in Figure 7a). Box plots show elevated p27pT157 (Figure 7a) and pSTAT3 (Figure 7b) correlated significantly with the levels of indicated proteins above the mean. Elevated pSTAT3pY705 levels correlate significantly with both p27pT157 ($R = 0.102$, $P = 0.006$) and with the activation of PI3K/mTOR effectors pAKT (pT308 and pT473), p70pT389, p90pT359, S6pS235 and S6pS240 ($R = 0.103$–0.428; P-values between 0.006 and $1.3E-10$) and correlated inversely with PTEN ($R = -0.10$, $P = 0.009$) (Figure 7b). Owing to the recent collection of TCGA samples, correlation with patient outcome was not possible. The correlation between pSTAT3 and PI3K/mTOR pathway activation was validated in a second data set of 712 primary breast cancers (AKTpS473, $R = 0.137$, $P = 0.0003$; mTORpS2448, $R = 0.172$, $P = 3.95E-06$). Unfortunately, p27pT157 and p27pT198 data were not available in the second breast cancer data set.

The strong correlation between activation of STAT3 and activation of multiple PI3K/mTOR pathway effector kinases was confirmed in over one thousand bladder, renal and lung cancers from TCGA data (Figure 7c). Patient follow-up time for these data sets was also too short to permit outcome analysis.

DISCUSSION

Distant metastases are the cause of most cancer patient deaths.[39] Despite substantial progress in our understanding of the complex process of human tumor metastasis, the lack of knowledge of molecular mechanisms underlying metastasis has limited our ability to specifically target tumor spread.[40] Cytoplasmic p27 acquires an oncogenic role, via RhoA-Rock inhibition, to increase cell migration.[15,41] Present data indicate that in addition to facilitating RhoA binding,[25] p27 phosphorylations at T157 and T198 link PI3K activation with an STAT3-driven metastatic cascade *in vivo* in human tumors. Knockdown of cellular p27 in PI3K-activated cancer models attenuates metastasis, whereas phosphomimetic p27CK-DD causes non-transformed mammary epithelial cells to acquire invasive ability *in vitro* and increases metastasis of cancer cells *in vivo*. Furthermore, we identify a mechanism in which C-terminally phosphorylated p27 drives tumor metastasis *in vivo* via STAT3 activation, which induces *TWIST1* and EMT.

To initiate metastasis, tumor cells must transgress cell–cell junctions and acquire the ability to invade beyond surrounding basement membranes.[42] Reactivation of EMT is thought to initiate this early step in the metastatic cascade.[33,38] Present data demonstrate that p27CK-DD is sufficient to induce a reversible, EMT-like phenotypic switch in two immortal, non-tumorigenic mammary epithelial lines, and to upregulate this process in tumorigenic cancer cells. Conversely, in PI3K-activated, metastatic 4175 breast and UMUC3-LuL2 bladder cancer models with high endogenous p27pT157pT198, p27 knockdown reverted the EMT phenotype, reduced cell invasion and substantially reduced the formation of experimental lung metastasis. The loss of metastatic ability following p27 knockdown in these models could not be attributed to effects on cell-cycle progression or proliferation. Thus, PI3K activation is accompanied by an oncogenic gain of function in which p27pT157pT198 promotes metastasis in part by trigging EMT-like changes. Cancer cells gain an advantage subverting a CDK inhibitor to promote tumor progression. This may explain why p27 is rarely completely lost, despite the decreased nuclear p27 observed in a majority of human cancers.[14,43]

EMT is initiated by several transcription factors, including Twist1, Snail and Slug.[44,45] Twist1 can act independently of Snail and Slug to repress E-cadherin and upregulate N-cadherin.[2] As a master regulator of embryonic morphogenesis, Twist1 has been shown to promote cancer metastasis by activating EMT.[45] Here, we show p27 knockdown in p27pT157pT198-enriched highly metastatic lines decreased *TWIST1* expression, whereas p27CK-DD transduction led to *TWIST1* overexpression in low metastatic cells. *TWIST1* knockdown reversed the p27CK-DD-induced mesenchymal phenotype, indicating *TWIST1* upregulation is key to p27CK-DD-induced EMT.

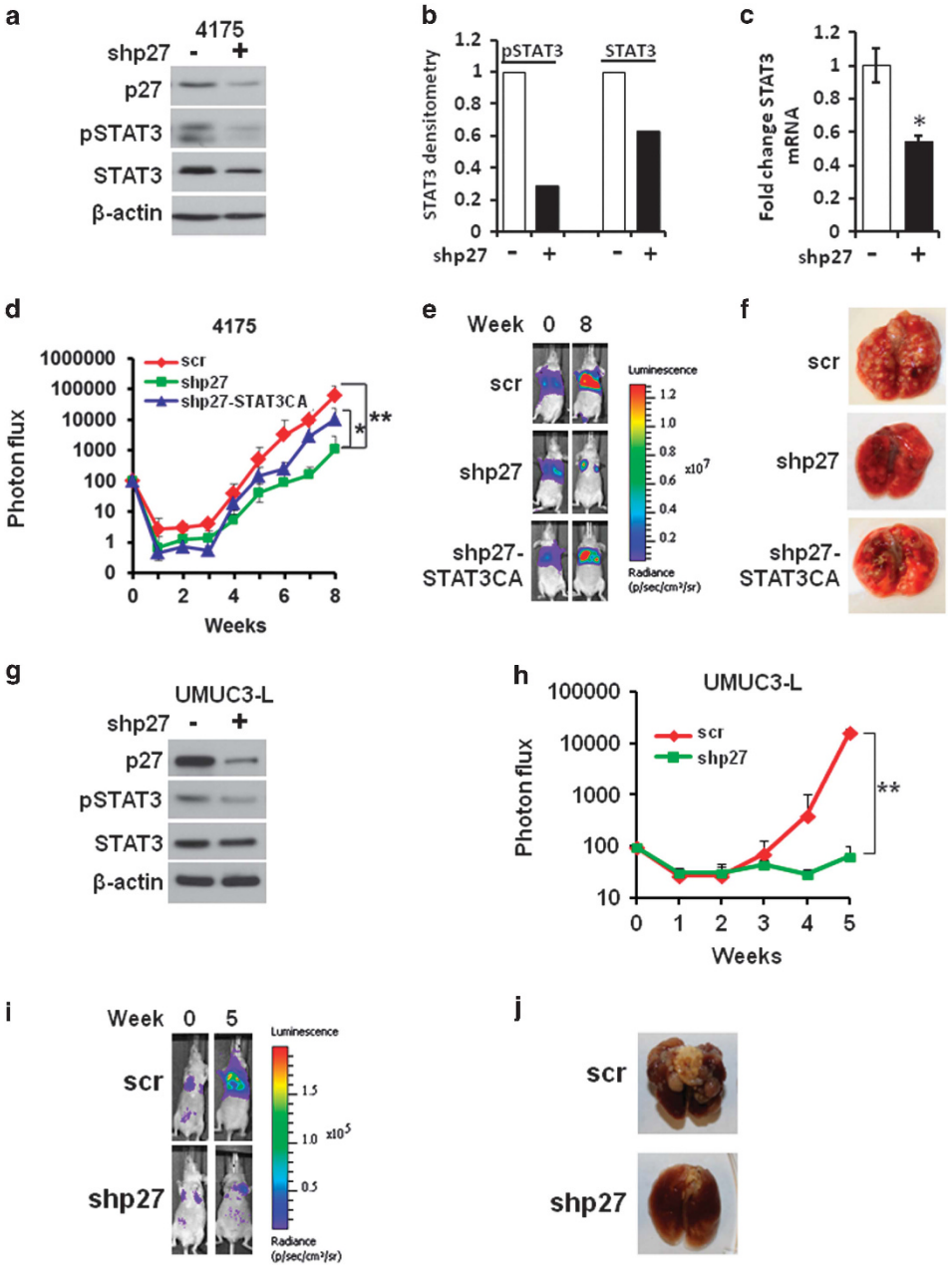

Figure 6. p27 knockdown reduces metastasis *in vivo* and is reversed by STAT3-CA. (**a**) Effects of p27 knockdown on STAT3 and pSTAT3 levels in 4175 cells. (**b**) Graphs of relative densitometry values from (**a**) for both pSTAT3 and total STAT3. (**c**) QPCR for *STAT3* mRNA in 4175 control and 4175shp27 cells. (**d**) Bioluminescence/time of experimental lung metastasis from xenograft mice that received intravenous injection of 4175 cells expressing the indicated vectors. (**e**) Representative bioluminescence imaging from indicated 4175 groups. The color scale depicts photon flux (photons/s) from xenografted mice. (**f**) Representative images of lungs from indicated 4175 groups. (**g**) Effects of p27 knockdown on STAT3 and pSTAT3 in UMUC3-LuL2 (UMUC3-L). (**h**) Bioluminescence/time of experimental lung metastasis from xenograft mice that received intravenous injection of UMUC3-L cells expressing indicated vectors. (**i**) Representative bioluminescence imaging from UMUC3-L groups. The color scale depicts photon flux (photons/s) from xenografted mice. (**j**) Representative images of lungs from indicated UMUC3-L groups. All data are graphed as mean ± s.e.m. $^{*}P < 0.05$ and $^{**}P < 0.01$.

STAT3 is aberrantly expressed and activated in many cancers including breast cancer[46] and has critical roles in malignant transformation and tumor progression.[47–49] p27 knockdown in p27pT157pT198-enriched cancer cells decreased total and phosphorylated STAT3. Conversely, p27CK-DD expression significantly increased total and phosphorylated STAT3 (Y705) in immortal mammary epithelial cells and cancer cells. STAT3 inhibition or STAT3DN reversed p27CK-DD-mediated EMT, reverted mesenchymal to epithelial morphology, upregulated epithelial markers and attenuated the p27CK-DD-mediated increases in cell invasion and cancer metastasis. Thus, STAT3 appears to be critical for the maintenance of p27-driven EMT and metastasis.

In cancer cells expressing high endogenous p27pT157pT198, we observed high TWIST1-luciferase activity and *TWIST1* expression. STAT3 inhibition and p27 knockdown, in 4175 cells, both attenuated *TWIST1* promoter activity and *TWIST1* expression, consistent with reports that *TWIST1* is induced by STAT3.[50,51] In both breast and bladder cancer models, p27CK-DD increased, whereas p27 knockdown decreased STAT3 occupancy and activation of the *TWIST1* promoter. p27 can act

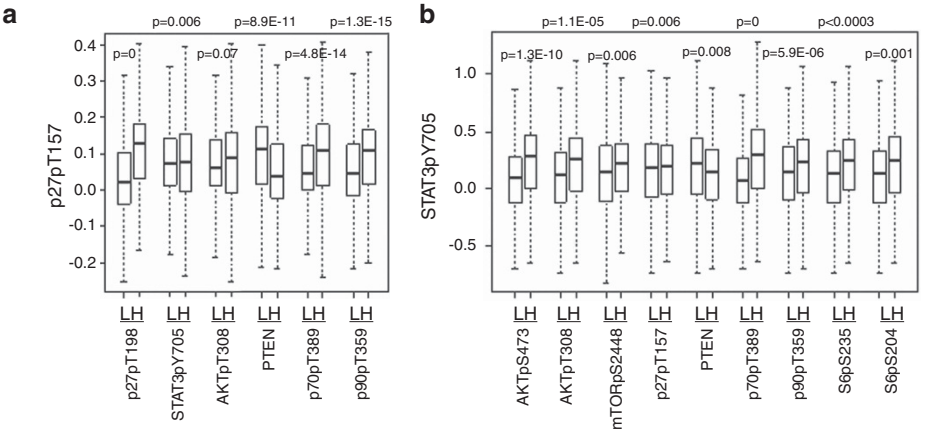

c Correlation of pSTAT3 with P13K/mTOR pathway activation

	Breast (n=747)		Bladder (n=127)		Kidney (n=454)		LungAD (n=237)		LungSQ (n=195)	
Kinase	R-value*	P-value	R-value	P-value	R-value	P-value	R-value	P-value	R-value	P-value
AKT pS473	0.238	1.29E-10	0.214	0.016	0.388	0	0.500	7.93E-03	0.211	0.003
mTOR pS2448	0.103	0.006	0.33	0.00015	0.205	1.11E-05	0.454	1.4E-10	0.35	5.94E-07
p70 pT389	0.428	0	NS		0.298	8.74E-11	NS		0.15	0.04
p90 pT359	0.169	5.94E-06	NS		0.158	0.0012	0.33	5.34E-06	0.124	0.09
S6 pS235	0.135	0.0003	NS		0.197	2.4E-05	0.300	4.34E-05	0.279	8.68E-05
S6 pS244	0.121	0.0001	NS		0.238	2.91E-07	0.309	2.27E-05	0.260	0.0002
PTEN	-0.098	0.009	NS		0.291	2.53E-10	NS		NS	

*R=correlation coefficient

Figure 7. Primary human cancers show significant associations between PI3K pathway activation, pSTAT3 and p27pT157. (**a** and **b**) RPPA analysis of 747 primary breast cancers from the TCGA/TCPA data set show significant Spearman's correlations between elevated p27pT157 (**a**) and STAT3pY705 (**b**), with each other and with PI3K pathway effectors shown. Box graphs depict tumors below and above 50th percentile expression for each variable as low (L) and high (H). Welch two-sample *t*-test was used to test significance. *P*-values for all data are shown. (**c**) Spearman's correlation analysis was performed between STAT3pY705 and the activated phosphorylation status of multiple PI3K/mTOR pathway effector kinases represented in the RPPA data in over 1000 cancers from the TCGA data sets, including breast, bladder, kidney and adeno (LungAD) and squamous lung (LungSQ) cancers is shown. n = number of tumors in the TCPA data set. NS, not significant; *R*-value, correlation coefficient.

in a cell-cycle-independent manner as a transcriptional corepressor with p130 and E2F4 to form a repressive complex at target promoters[52,53] and p27 has been shown to form part of a *TWIST1* repressor complex.[54] Although it is tempting to speculate that C-terminal phosphorylation of p27 might sterically disrupt repressive complexes at certain promoters and convert p27 from a corepressor to a coactivator at novel gene promoters, we were unable to detect p27 in complex with STAT3 on the *TWIST1* promoter. p27CK-DD transduction led to the formation of a tripartite p27/JAK2/STAT3 complex and increased JAK2-bound STAT3 and STAT3 activation. In addition, cellular p27pT198 co-precipitates STAT3 and JAK2/STAT3/p27 complexes were increased in 4175 cells compared with 231 cells and were attenuated by PI3K inhibition. These data suggest a model in which p27pT157pT198 binds JAK2 to facilitate STAT3 recruitment and activation, and STAT3-dependent *TWIST1* induction.

Present data also reveal a feedforward loop between PI3K, p27 and STAT3. p27CK-DD-expressing cells showed a STAT3-dependent increase in AKT activation. Our proteomic analysis of two independent breast cancer data sets comprising over 1400 primary cancers and additional TCGA/TCPA data sets of over 1000 primary cancers of bladder, kidney and lung all show correlations between pSTAT3 and PI3K pathway activation, supporting our *in vitro* and *in vivo* findings. Thus, PI3K activation in human cancer would increase p27 phosphorylation at T157 and T198 to promote a STAT3/*TWIST1*-dependent EMT. In addition, p27pT157pT198 would also drive STAT3-dependent AKT activation, to further phosphorylate p27, amplify STAT3 activation and drive EMT.

In summary, we have uncovered a novel oncogenic function of p27 to drive tumor metastasis through the activation of EMT in both breast and bladder cancer models. Cytoplasmic p27 is observed in many human cancers[12] and is correlated with adverse outcome in prostate cancer,[55] renal cell cancer,[56] glioma[57] and high-grade astrocytomas.[58] In breast cancer, cytoplasmic p27 staining correlates with AKT activation,[19,20,59] predicts early disease relapse[59] and is associated with increased lymph nodal metastasis and poor overall survival.[29] Our analysis of proteomic data in primary human breast cancers also links PI3K/mTOR activation with high p27pT157 and reveals a novel association with activated pSTAT3. Taken together, these data support an oncogenic feedforward loop in which oncogenic PI3K activation would increase p27pT157pT198 to increase STAT3 activity, further activate AKT, induce STAT3-dependent *TWIST1* expression and drive EMT, contributing thereby to the acquisition and maintenance of metastatic potential. Combined inhibition of PI3K/mTOR and JAK2/STAT3 in p27pT157pT198-enriched human cancers may ultimately have therapeutic potential to limit p27-mediated EMT and cancer metastasis.

MATERIALS AND METHODS

Cell lines and reagents

The immortalized human mammary epithelial MCF-12A cell lines (ATCC Manassas, VA, USA) and HME3 cell lines were cultured as described.[32] MDA-MB-231-luc and MDA-MB-4175-luc cells (from J Massague, MSKCC, New York, NY, USA)[34] and MCF-7 cells were cultured in Dulbecco's modified Eagle's medium with 10% fetal bovine serum. Bladder cancer lines UMUC3 and UMUC3-LuL2[35] were cultured in Iscove's modified Eagle's medium with 10% fetal bovine serum. Lenti-X 293T cells from Clontech (Mountain View, CA, USA) were cultured in Dulbecco's modified Eagle's medium with 10% fetal bovine serum.

Reagents were obtained as follows: lentivirus vector Plvx-AcGFP (from Clontech); lenti-STAT3DN (from Addgene, Cambridge, MA, USA); pBabe-STAT3-CA (from J Bromberg; MSKCC); PI3K/mTOR inhibitor PF-04691502 (used at 250 nM) (from Pfizer, New York, NY, USA); 5, 15-diphenylporphyrin (used at 50 μM) to inhibit STAT3 (from Calbiochem, Billerica, MA, USA); and short hairpin RNAs of p27 and *TWIST1* (from Open Biosystems, GE Dharmacon, Lafayette, CO, USA).

p27 mutants

Phosphomimetic p27 mutations were introduced into EGFP-p27CK$-^{30}$ (from S Dowdy, UCSD, La Jolla, CA, USA) by site-directed mutagenesis and subcloned into Plvx-AcGFP to generate Plvx-AcGFP-p27CK- and Plvx-AcGFP-p27CK-DD vectors for virus packaging to infect target cells.

Lentivirus production and stable line generation

Details of the generation of cells expressing lentivirus vectors encoding three different short hairpin RNAs to *CDKN1B* (p27) and *TWIST1* (Open Biosystems) or Plvx-AcGFP and Plvx-AcGFP-p27CK-DD are in given in the Supplementary Information.

Transwell migration and invasion assay

A total of 2×10^4 cells were seeded for transwell migration assays and 10^5 cells were seeded for invasion assays into either modified Boyden chambers or automated transwell assays using the Real-Time Cell Analysis system from Xcelligence (ACEA Biosciences, San Diego, CA, USA)[29] (see Supplementary Information for details).

Quantitative real-time PCR and siRNA analysis

Quantitative real-time PCR (QPCR) analyses were performed in triplicate as described[29] and average C_t values were normalized to *GAPDH* values (see Supplementary Methods for primer sequences). SiRNAs consisting of pools of three to five target-specific 19–25 nucleotide siRNAs to *p27* and scrambled controls were purchased from Santa Cruz Biotechnology (Dallas, TX, USA) and used as per the manufacturer's instructions.

Western blotting

Western blots were performed as described.[25] Antibodies used in western blots were as follows: anti-pAKT S473, AKT, pPDK1 S241, PDK1, pSTAT3 Y705 and STAT3 (from Cell Signaling); for E-cadherin, N-cadherin and p27 from Transduction Labs; and for p27pT157 and p27pT198 from R&D Systems. p27 immunoprecipitation used PAb C-19 from Santa Cruz Biotechnology.

Drug treatment

MCF-12A-p27CK-DD cells were treated with or without STAT3 inhibitor 5, 15-diphenyporphyrin (50 μM) for 2 weeks before fluorescence immunocytochemistry, cell invasion and western blot analysis. MDA-MB-4175 cells were treated with or without PI3K/mTOR inhibitor PF-04691502 (250 nM) for one day before p27 or JAK2 immunoprecipitations.

Fluorescence immunocytochemistry

Fluorescence immunocytochemistry was performed as described.[21] Primary antibodies used were: E-cadherin (1:1000), N-cadherin (1:500), vimentin (1:500), pSTAT3 (1:1000) and Twist1 (1:500), followed by incubation with Alexa Fluor 594-conjugated secondary antibody (1:200). Nuclei were stained with 4',6-diamidino-2-phenylindole, and cells were mounted in Prolong Gold antifade reagent (Invitrogen). Photomicrographs were taken using a Zeiss Axiovert microscope (Zeiss, Jena, Germany).

Immunoprecipitation

MDA-MB-231 and 4175 cells treated with or without PF-04691502 (250 nM) for 24 h were lysed, and 2 mg lysate from MDA-MB-231 cells and 1 mg lysate from 4175 cells were incubated with 1 μg of p27 antibody (C-19; Santa Cruz Biotechnology), collected on protein G-agarose and washed three times with IP buffer and then analyzed by western blot for bound STAT3 and p27. Antibody-alone controls were run with all immunoprecipitations.

Chromatin immunoprecipitation assay

ChIP assays for STAT3 on *TWIST1* promoter were as described.[52] MDA-MB-231 and UMUC3 cells expressing control vector or p27CK-DD, or p27CK-DD-STAT3DN, 4175scr, 4175shp27, UMUC3-LuL2scr and UMUC3-LuL2shp27 cells were serum deprived and then replenished with media plus 20 ng/ml epidermal growth factor for 1 h followed by ChIP assays (see Supplementary Methods for details).

Human phosphokinase array

To determine which phosphokinases are changed by p27CK-DD expression, MCF-12A-GFP and MCF-12A-p27CK-DD cells were assayed using a human phospho-kinome array (ARY003, Proteome Profiler; R&D Systems, Minneapolis, MN, USA) as per the manufacturer's protocol.

This kit tests over 43 phosphokinases. For a complete list of the antibodies in this array, please see the following link: http://www.rndsystems.com/product_detail_objectname_kinaseantibodyarray.aspx.

Luciferase assay

Cells were seeded at 5000 cells per well in an opaque 96-well plate. After 24 h, cells were transfected with 50 ng of *TWIST1* promoter or control promoter luciferase vector (SwitchGear Genomics, Menlo Park, CA, USA) using Fugene-6 (Roche, San Francisco, CA, USA). Luciferase activity was assayed 24 h later, using LightSwitch Assay Reagent (SwitchGear Genomics) and a GloMax-Multi+ Detection System with Instinct Software (Promega, Madison, WI, USA). Relative luciferase expression was calculated as a percent maximum of the highest sample in each group.

Experimental metastasis assay

MDA-MB-231-luc cells (5×10^5) expressing AcGFP, p27CK-DD or p27CK-DD-STAT3DN and 2×10^5 MDA-MB-4175-luc cells with scr, shp27 or shp27-STAT3-CA were injected via the tail vein into 4–6-week-old female Balb/C nude mice (Charles River Laboratories, Wilmington, MA, USA). UMUC3 cells (2×10^6) expressing AcGFP, p27CK-DD or p27CK-DD-STAT3DN and UMUC3-LuL2 cells expressing scr or shp27 were injected via the tail vein into a 6-week-old female athymic (nu^+/nu^+) mice (NCI, Bethesda, MD, USA) (see Supplementary Methods for additional details).

Bioluminescence imaging and analysis

Mice were anesthetized and injected intraperitoneally with 1.5 mg of D-luciferin (15 mg/ml in phosphate-buffered saline) and imaged using Xenogen IVIS system (Xenogen, Caliper, Hopkinton, MA, USA) as in Wander *et al*.[29] Values were normalized to those obtained immediately after xenografting (day 0) so that all mice had an arbitrary starting bioluminescence signal of 100. Average normalized photon flux is plotted over time ± s.e.m. Representative individual mice were photographed and presented along with a standardized scale.

Reverse-phase protein array analysis of human tumors

Reverse-phase protein array (RPPA) assay was performed at the Functional Proteomics Reverse Phase Protein Array Core facility at MD Anderson to test the expression of 178 proteins and phosphoproteins in 747 breast cancers from TCGA project as described.[60] RPPA data processing used SuperCurve (Coombes K, *et al*., SuperCurve: SuperCurve Package, R package version 1.4.1.2011) as described.[60] The protein expression data (RPPA) for breast, lung, kidney and bladder cancers samples were downloaded from the TCPA website (http://bioinformatics.mdanderson.org/main/TCPA). For detailed RPPA method, see Supplementary Information.

Statistical analysis

All graphed data are from at least three experiments and presented as means ± s.e. Two-tailed Student's *t*-tests were used to test differences. *P*-values < 0.05 were considered statistically significant. The statistical differences between curves were calculated using 'compareGrowthCurves' function of the StatMod software (http://bioinf.wehi.edu.au/software/compareCurves) for IVIS metastatic tumor growth curves.

To test the correlations between pSTAT3, p27pT157 and activation of PI3K/mTOR pathway kinases in the RPPA data, Spearman's correlation analysis was performed between pairs of protein levels among proteins represented in the RPPA data. *P*-values within boxplots were determined using the Welch two-sample *t*-test.

CONFLICT OF INTEREST

The authors declare no conflict of interest.

ACKNOWLEDGEMENTS

We acknowledge the support of lab members, the UMSCCC Analytical Imaging Core Facility and Grant NCI-2R01CA105118-05A. A grant from the Doris Duke Charitable Foundation supported AB, SW and JMS.

REFERENCES

1 Sethi N, Kang Y. Unravelling the complexity of metastasis—molecular understanding and targeted therapies. *Nat Rev Cancer* 2011; **11**: 735–748.
2 Thiery JP, Acloque H, Huang RY, Nieto MA. Epithelial–mesenchymal transitions in development and disease. *Cell* 2009; **139**: 871–890.
3 Kim MY, Oskarsson T, Acharyya S, Nguyen DX, Zhang XH, Norton L *et al.* Tumor self-seeding by circulating cancer cells. *Cell* 2009; **139**: 1315–1326.
4 Slingerland JM, Hengst L, Pan CH, Alexander D, Stampfer MR, Reed SI. A novel inhibitor of cyclin-Cdk activity detected in transforming growth factor beta-arrested epithelial cells. *Mol Cell Biol* 1994; **14**: 3683–3694.
5 Hengst L, Dulic V, Slingerland JM, Lees E, Reed SI. A cell cycle-regulated inhibitor of cyclin-dependent kinases. *Proc Natl Acad Sci USA* 1994; **91**: 5291–5295.
6 Koff A, Ohtsuki M, Polyak K, Roberts JM, Massague J. Negative regulation of G1 in mammalian cells: inhibition of cyclin E-dependent kinase by TGF-beta. *Science* 1993; **260**: 536–539.
7 Polyak K, Kato JY, Solomon MJ, Sherr CJ, Massague J, Roberts JM *et al.* P27Kip1, a cyclin-Cdk inhibitor, links transforming growth factor-beta and contact inhibition to cell cycle arrest. *Genes Dev* 1994; **8**: 9–22.
8 Kiyokawa H, Kineman RD, Manova-Todorova KO, Soares VC, Hoffman ES, Ono M *et al.* Enhanced growth of mice lacking the cyclin-dependent kinase inhibitor function of p27Kip1. *Cell* 1996; **85**: 721–732.
9 Nakayama K, Ishida N, Shirane M, Inomata A, Inoue T, Shishido N *et al.* Mice lacking p27(Kip1) display increased body size, multiple organ hyperplasia, retinal dysplasia, and pituitary tumors. *Cell* 1996; **85**: 707–720.
10 Fero ML, Rivkin M, Tasch M, Porter P, Carow CE, Polyak K *et al.* A syndrome of multi-organ hyperplasia with features of gigantism, tumorigenesis and female sterility in p27Kip1-deficient mice. *Cell* 1996; **85**: 733–744.
11 Fero ML, Randel E, Gurley KE, Roberts JM, Kemp CJ. The murine gene p27Kip1 is haplo-insufficient for tumour suppression. *Nature* 1998; **396**: 177–180.
12 Chu IM, Hengst L, Slingerland JM. The Cdk inhibitor p27 in human cancer: prognostic potential and relevance to anticancer therapy. *Nat Rev Cancer* 2008; **8**: 253–267.
13 Slingerland J, Pagano M. Regulation of the cdk inhibitor p27 and its deregulation in cancer. *J Cell Physiol* 2000; **183**: 10–17.
14 Besson A, Dowdy SF, Roberts JM. CDK inhibitors: cell cycle regulators and beyond. *Dev Cell* 2008; **14**: 159–169.
15 Besson A, Gurian-West M, Schmidt A, Hall A, Roberts JM. P27Kip1 modulates cell migration through the regulation of RhoA activation. *Genes Dev* 2004; **18**: 862–876.
16 Besson A, Assoian RK, Roberts JM. Regulation of the cytoskeleton: an oncogenic function for CDK inhibitors? *Nat Rev Cancer* 2004; **4**: 948–955.
17 Nagahara H, Vocero-Akbani AM, Synder EL, Ho A, Latham DG, Lissy NA *et al.* Transduction of full-length TAT fusion proteins into mammalian cells: TAT-p27Kip1 induces cell migration. *Nat Med* 1998; **4**: 1449–1452.
18 Liang J, Zubovitz J, Petrocelli T, Kotchetkov R, Connor MK, Han K *et al.* PKB/Akt phosphorylates p27, impairs nuclear import of p27 and opposes p27-mediated G1 arrest. *Nat Med* 2002; **8**: 1153–1160.
19 Shin I, Yakes FM, Rojo F, Shin NY, Bakin AV, Baselga J *et al.* PKB/Akt mediates cell-cycle progression by phosphorylation of p27(Kip1) at threonine 157 and modulation of its cellular localization. *Nat Med* 2002; **8**: 1145–1152.
20 Viglietto G, Motti ML, Bruni P, Melillo RM, D'Alessio A, Califano D *et al.* Cytoplasmic relocalization and inhibition of the cyclin-dependent kinase inhibitor p27(Kip1) by PKB/Akt-mediated phosphorylation in breast cancer. *Nat Med* 2002; **8**: 1136–1144.
21 Hong F, Larrea MD, Doughty C, Kwiatkowski DJ, Squillace R, Slingerland JM. mTOR-raptor binds and activates SGK1 to regulate p27 phosphorylation. *Mol Cell* 2008; **30**: 701–711.
22 Fujita N, Sato S, Katayama K, Tsuruo T. Akt-dependent phosphorylation of p27Kip1 promotes binding to 14-3-3 and cytoplasmic localization. *J Biol Chem* 2002; **277**: 28706–28713.
23 Motti ML, De Marco C, Califano D, Fusco A, Viglietto G. Akt-dependent T198 phosphorylation of cyclin-dependent kinase inhibitor p27(kip1) in breast cancer. *Cell Cycle* 2004; **3**: 1074–1080.
24 Fujita N, Sato S, Tsuruo T. Phosphorylation of p27Kip1 at threonine 198 by p90 ribosomal protein S6 kinases promotes its binding to 14-3-3 and cytoplasmic localization. *J Biol Chem* 2003; **278**: 49254–49260.
25 Larrea MD, Hong F, Wander SA, da Silva TG, Helfman D, Lannigan D *et al.* RSK1 drives p27Kip1 phosphorylation at T198 to promote RhoA inhibition and increase cell motility. *Proc Natl Acad Sci USA* 2009; **106**: 9268–9273.
26 Liang J, Shao SH, Xu Z, Hennessy B, Ding Z, Larrea M *et al.* The energy sensing LKB1-AMPK pathway regulates p27(kip1) phosphorylation mediating the decision to enter autophagy or apoptosis. *Nat Cell Biol* 2007; **9**: 218–224.
27 Kossatz U, Vervoorts J, Nickeleit I, Sundberg HA, Arthur JSC, Manns MP *et al.* C-terminal phosphorylation controls the stability and function of p27kip1. *EMBO J* 2006; **25**: 5159–5170.
28 Serres MP, Zlotek-Zlotkiewicz E, Concha C, Gurian-West M, Daburon V, Roberts JM *et al.* Cytoplasmic p27 is oncogenic and cooperates with Ras both *in vivo* and *in vitro*. *Oncogene* 2011; **30**: 2846–2858.
29 Wander S, Zhao D, Besser A, Hong F, Wei J, Ince T *et al.* PI3K/mTOR inhibition can impair tumor invasion and metastasis *in vivo* despite a lack of antiproliferative action *in vitro*: implications for targeted therapy. *Breast Cancer Res Treat* 2013; **138**: 369–381.
30 Denicourt C, Saenz CC, Datnow B, Cui XS, Dowdy SF. Relocalized p27(KiP1) tumor suppressor functions as a cytoplasmic metastatic oncogene in melanoma. *Cancer Res* 2007; **67**: 9238–9243.
31 Vlach J, Hennecke S, Amati B. Phosphorylation-dependent degradation of the cyclin-dependent kinase inhibitor p27. *EMBO J* 1997; **16**: 5334–5344.
32 Ince TA, Richardson AL, Bell GW, Saitoh M, Godar S, Karnoub AE *et al.* Transformation of different human breast epithelial cell types leads to distinct tumor phenotypes. *Cancer Cell* 2007; **12**: 160–170.
33 Puisieux A, Brabletz T, Caramel J. Oncogenic roles of EMT-inducing transcription factors. *Nat Cell Biol* 2014; **16**: 488–494.
34 Minn AJ, Gupta GP, Siegel PM, Bos PD, Shu W, Giri DD *et al.* Genes that mediate breast cancer metastasis to lung. *Nature* 2005; **436**: 518–524.
35 Nitz MD, Harding MA, Theodorescu D. Invasion and metastasis models for studying RhoGDI2 in bladder cancer. *Methods Enzymol* 2008; **439**: 219–233.
36 Jakel H, Weinl C, Hengst L. Phosphorylation of p27Kip1 by JAK2 directly links cytokine receptor signaling to cell cycle control. *Oncogene* 2011; **30**: 3502–3512.
37 Kalluri R, Weinberg RA. The basics of epithelial–mesenchymal transition. *J Clin Invest* 2009; **119**: 1420–1428.
38 Micalizzi DS, Farabaugh SM, Ford HL. Epithelial–mesenchymal transition in cancer: parallels between normal development and tumor progression. *J Mamm Gland Biol Neoplasia* 2010; **15**: 117–134.
39 Valastyan S, Weinberg RA. Tumor metastasis: molecular insights and evolving paradigms. *Cell* 2011; **147**: 275–292.
40 Chiang AC, Massague J. Molecular basis of metastasis. *N Engl J Med* 2008; **359**: 2814–2823.
41 Besson A, Hwang HC, Cicero S, Donovan SL, Gurian-West M, Johnson D *et al.* Discovery of an oncogenic activity in p27Kip1 that causes stem cell expansion and a multiple tumor phenotype. *Genes Dev* 2007; **21**: 1731–1746.
42 Chaffer CL, Weinberg RA. A perspective on cancer cell metastasis. *Science* 2011; **331**: 1559–1564.
43 Wander SA, Zhao D, Slingerland JM. P27: a barometer of signaling deregulation and potential predictor of response to targeted therapies. *Clin Cancer Res* 2011; **17**: 12–18.
44 Ansieau S, Morel AP, Hinkal G, Bastid J, Puisieux A. TWISTing an embryonic transcription factor into an oncoprotein. *Oncogene* 2010; **29**: 3173–3184.
45 Yang J, Mani SA, Donaher JL, Ramaswamy S, Itzykson RA, Come C *et al.* Twist, a master regulator of morphogenesis, plays an essential role in tumor metastasis. *Cell* 2004; **117**: 927–939.
46 Lieblein JC, Ball S, Hutzen B, Sasser AK, Lin HJ, Huang TH *et al.* STAT3 can be activated through paracrine signaling in breast epithelial cells. *BMC Cancer* 2008; **8**: 302.
47 Marotta LL, Almendro V, Marusyk A, Shipitsin M, Schemme J, Walker SR *et al.* The JAK2/STAT3 signaling pathway is required for growth of $CD44^+CD24^-$ stem cell-like breast cancer cells in human tumors. *J Clin Invest* 2011; **121**: 2723–2735.
48 Devarajan E, Huang S. STAT3 as a central regulator of tumor metastases. *Curr Mol Med* 2009; **9**: 626–633.
49 Xiong H, Hong J, Du W, Lin YW, Ren LL, Wang YC *et al.* Roles of STAT3 and ZEB1 proteins in E-cadherin down-regulation and human colorectal cancer epithelial-mesenchymal transition. *J Biol Chem* 2012; **287**: 5819–5832.
50 Cheng GZ, Zhang WZ, Sun M, Wang Q, Coppola D, Mansour M *et al.* Twist is transcriptionally induced by activation of STAT3 and mediates STAT3 oncogenic function. *J Biol Chem* 2008; **283**: 14665–14673.
51 Lo HW, Hsu SC, Xia W, Cao X, Shih JY, Wei Y *et al.* Epidermal growth factor receptor cooperates with signal transducer and activator of transcription 3 to induce epithelial–mesenchymal transition in cancer cells via up-regulation of TWIST gene expression. *Cancer Res* 2007; **67**: 9066–9076.

52 Li H, Collado M, Villasante A, Matheu A, Lynch CJ, Canamero M *et al.* P27(Kip1) directly represses Sox2 during embryonic stem cell differentiation. *Cell Stem Cell* 2012; **11**: 845–852.
53 Pippa R, Espinosa L, Gundem G, Garcia-Escudero R, Dominguez A, Orlando S *et al.* P27Kip1 represses transcription by direct interaction with p130/E2F4 at the promoters of target genes. *Oncogene* 2012; **31**: 4207–4220.
54 Menchon C, Edel MJ, Izpisua Belmonte JC. The cell cycle inhibitor p27Kip(1) controls self-renewal and pluripotency of human embryonic stem cells by regulating the cell cycle, Brachyury and Twist. *Cell Cycle* 2011; **10**: 1435–1447.
55 Li R, Wheeler TM, Dai H, Sayeeduddin M, Scardino PT, Frolov A *et al.* Biological correlates of p27 compartmental expression in prostate cancer. *J Urol* 2006; **175**: 528–532.
56 Kruck S, Merseburger AS, Hennenlotter J, Scharpf M, Eyrich C, Amend B *et al.* High cytoplasmic expression of p27(Kip1) is associated with a worse cancer-specific survival in clear cell renal cell carcinoma. *BJU Int* 2012; **109**: 1565–1570.
57 Piva R, Cancelli I, Cavalla P, Bortolotto S, Dominguez J, Draetta GF *et al.* Proteasome-dependent degradation of p27/kip1 in gliomas. *J Neuropathol Exp Neurol* 1999; **58**: 691–696.
58 Hidaka T, Hama S, Shrestha P, Saito T, Kajiwara Y, Yamasaki F *et al.* The combination of low cytoplasmic and high nuclear expression of p27 predicts a better prognosis in high-grade astrocytoma. *Anticancer Res* 2009; **29**: 597–603.
59 Liang J, Han K, Hung W, Slingerland JM. Akt/PKB-dependent phosphorylation of p27 activates the cylin D1/Cdk4 assembly function of p27 and G1 cell cycle progression. *Cold Spring Harbor Cell Cycle Meet* **3**2002.
60 Hennessy BT, Lu Y, Gonzalez-Angulo AM, Carey MS, Myhre S, Ju Z *et al.* A technical assessment of the utility of reverse phase protein arrays for the study of the functional proteome in non-microdissected human breast cancers. *Clin Proteom* 2010; **6**: 129–151.

Supplementary Information accompanies this paper on the Oncogene website (http://www.nature.com/onc)